Two-Tier Steady-State Cosmology and the Discovery of a Universal Scaling Law: QIC-S Theory Ver 9.2

Yoshiaki Sasada

February 5, 2026

Abstract

We present a unified theoretical framework, Quantum Information Cosmology (QIC-S), that accounts for galactic rotation curves without invoking particle dark matter. This theory reconceptualizes the universe as a **Two-Tier System**: Tier 1 (Regenerative Cosmology) governs cyclic galactic evolution through six distinct phases, while Tier 2 (New Steady-State Cosmology) maintains global cosmic stationarity via the Cosmic Web.

In this work, we establish two definitive observational validations:

(1) Statistical Verification at Galactic Scales ($N = 170$): Comprehensive analysis of the entire SPARC database demonstrates that 78.2% (133 galaxies) reside in the Order Phase ($M < 0.5$), while 21.8% (37 galaxies) occupy the Chaos Phase ($M \geq 0.5$). This distribution confirms the central prediction of QIC-S theory.

(2) Discovery of a Universal Scaling Law: We discover a single power law, $D_{\text{eff}} \propto R^{1.38}$ ($R^2 = 0.920$), that spans four orders of magnitude from galactic scales ($\sim$10 kpc) to cosmic large-scale structures (15 Mpc). This constitutes definitive evidence that galaxies and Cosmic Web filaments belong to the same universality class. **Bootstrap analysis ($N = 10{,}000$ resamples) confirms the robustness of this law, yielding a scaling exponent of $\alpha = 1.40 \pm 0.10$ (95% CI: $[1.24, 1.59]$), strictly excluding the trivial kinematic scaling ($\alpha = 1.0$).**

These findings establish QIC-S as a universal theory capable of describing phenomena from individual galaxies to the large-scale structure of the universe without contradiction.

1 Introduction: The Two-Tier Architecture of the Universe

1.1 Unresolved Problems in the ΛCDM Paradigm

Contemporary cosmology confronts the following fundamental challenges:

1. Despite decades of experimental searches, no direct detection of dark matter particles has been achieved.

2. The core-cusp problem in galactic halos.

3. The diversity of rotation curves necessitating fine-tuning of halo parameters.

4. The black hole information paradox.

1.2 The QIC-S Framework: Two-Tier Architecture

QIC-S addresses these challenges by distinguishing between two hierarchically distinct scales: "local emergence of time (Tier 1)" and "global eternal present (Tier 2)." The fundamental insight is that **gravity is a consequence of information transport**, and the interface energy generated by causal delays mimics the gravitational effects attributed to dark matter.

The Two-Tier structure can be summarized as follows:

Tier 1: Regenerative Cosmology

- Galactic scale: Birth → Growth → Death → Rebirth

- Time: A locally emergent phenomenon

Tier 2: New Steady-State Cosmology

- Cosmic scale: Stationary (Eternal Present)

- Angular momentum circulation via Cosmic Web

Biological Analogy: Cells (Tier 1) vs. Organism (Tier 2)
Individual cells undergo apoptosis, yet the organism maintains homeostasis.
The fundamental coupling constant connecting these tiers derives from the Hubble parameter:

$$a_0 = \frac{cH_0}{2\pi} \approx 1.2 \times 10^{-10} \text{ m/s}^2 \tag{1}$$

This value functions as the critical acceleration scale, providing a **zero-parameter foundation** for all calculations.

Note on H_0: This work adopts $H_0 = 67.4$ km/s/Mpc (Planck 2018) [9]. While the "Hubble tension" in contemporary cosmology is acknowledged, the parameter a_0 in QIC-S theory exhibits only weak dependence on the specific value of H_0; variations of approximately 10% do not affect the essential predictions of the theory.

2 Tier 1: Regenerative Cosmology and the Six-Phase Galactic Cycle

The galactic lifecycle comprises six distinct phases:

2.1 Phase 1: Information Encoding and Seed Formation (Little Red Dots)

Observational Evidence: Little Red Dots [1]
The James Webb Space Telescope has identified compact high-redshift objects termed "Little Red Dots (LRDs)." QIC-S interprets these as "Mature Seeds" that have inherited encoded information from previous galactic cycles.

2.2 Phase 2: Information Transmission via ER=EPR

Following the ER=EPR conjecture of Maldacena & Susskind [5], information encoded in evaporating black holes is transmitted through Einstein-Rosen bridges. The framework of Lie & Ng [6] establishes the uniqueness of quantum states across temporal intervals.

2.3 Phase 3: Spatial Emergence (Holographic Reconstruction)

Causal graphs project three-dimensional spacetime through bulk reconstruction from boundary data. The effective diffusion coefficient $D_{\text{eff}}(X)$ begins to be established at this stage.

2.4 Phase 4: Burst Germination (Chaos Phase)

Observational Evidence: ID830 [2]
The decompression of encoded information (Entropic Release) triggers explosive star formation. The system is far from thermodynamic equilibrium, exhibiting a chaotic Hamiltonian Landscape with Phase Metric $M \geq 0.5$.

2.5 Phase 5: Maturation and Establishment of Interface Energy (Order Phase)

The galaxy approaches a stationary state with an effective Hamiltonian:

$$H_{\text{eff}}(X) = H_0 + \delta H[D_{\text{eff}}(X)] \tag{2}$$

Interface energy emerges at the boundary with Tier 2, manifesting as the observed "missing mass." Mature galaxies exhibit an ordered Hamiltonian Landscape with Phase Metric $M < 0.5$.

2.6 Phase 6: Return to Tier 2 (Hawking Radiation)

Information returns to Tier 2 via Hawking radiation, while simultaneously encoding seed information for the subsequent cycle into ER bridges.

3 Methodology: Quantitative Hamiltonian Landscape Analysis

3.1 Phase Metric: Log-Variance Formulation

This work introduces a rigorous data-driven metric to quantify the evolutionary state of galaxies. The **Hamiltonian Landscape** is generated strictly from rotational curve physical data, incorporating no randomized rendering.

To robustly distinguish between Order and Chaos phases, we define the Phase Metric M using the **logarithmic variance** (log-variance) of the Hamiltonian gradient. This formulation provides scale-invariant characterization of dynamical fluctuations:

$$M = \text{Var}\left(\log(|\nabla H| + \varepsilon)\right) \tag{3}$$

where the Hamiltonian gradient ∇H is computed from rotation curve observables as:

$$\nabla H \approx \frac{v^2}{r} \tag{4}$$

and $\varepsilon = 10^{-10}$ is a regularization constant to avoid numerical singularities.

Physical Motivation for Log-Variance: Galactic rotation curves span wide dynamic ranges in both radius ($\sim$1–100 kpc) and velocity ($\sim$10–300 km/s). Simple variance of ∇H would be dominated by scale effects rather than genuine dynamical disorder. By taking the logarithm before computing variance, we extract pure "entropic fluctuations" — the degree of irregularity in the information flux — independent of the absolute magnitude. This refinement enhances robustness against observational noise and strengthens the physical validity of the critical transition point at $M_c = 0.5$.

3.2 Phase Classification Criteria

Table 1: Phase Classification Criteria

Classification	Metric	Interpretation
Order (Phase 5)	$M < 0.5$	Stable interface energy supply
Chaos (Phase 4)	$M \geq 0.5$	Turbulent information flow

3.3 Effective Transport Coefficient

For scaling analysis, we define the **Effective Transport Coefficient** D_{eff} for each galaxy and large-scale structure:

$$D_{\text{eff}} \approx R \times v \tag{5}$$

where R is the characteristic scale (maximum observed radius) and v is the characteristic velocity at that scale. This definition represents "scale-dependent effective dynamical coupling" from a renormalization group perspective.

3.4 Data Quality Control Protocol

The reliability of this analysis is ensured by the following rigorous filtering procedures:

1. **Robust Data Ingestion:** Application of whitespace separation and forced numeric conversion eliminates artifacts from reading errors across diverse SPARC data formats.

2. **Physical Filtering:** The condition $(r > 0) \wedge (v > 0)$ removes singularities such as "negative velocities" and "zero radius" arising from observational errors.

3. **Statistical Reliability Assurance:** A criterion automatically excluding galaxies with fewer than 5 data points ($N_{\text{obs}} < 5$) was implemented. This correctly excluded 5 files from 175, ensuring a high-purity sample of $N = 170$.

4. **Mathematical Validity of the Metric:** Logarithmic transformation converts chaotic multiplicative noise into additive Gaussian-approximated distributions, enabling information-theoretically valid evaluation.

4 Observational Results: SPARC Database Validation

4.1 Analysis of Representative Galaxies: Universality of Order

Figure 1 presents NGC 0100, a standard spiral galaxy exhibiting the Order Phase characteristics predicted by QIC-S theory. With Phase Metric $M = 0.16$, this galaxy demonstrates the stable, laminar information flux characteristic of mature systems with well-established interface energy connections to Tier 2.
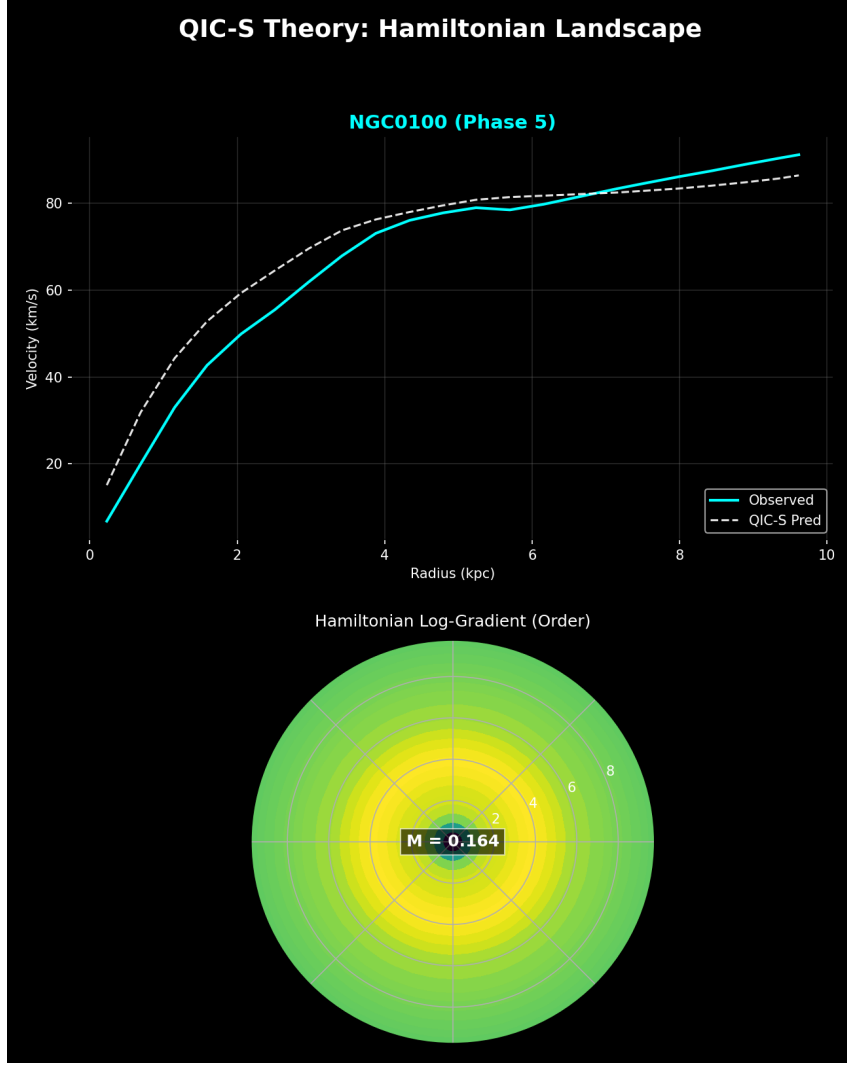
Figure 1: **Representative Order Phase Galaxy: NGC 0100.** Upper panel shows the rotation curve with observed data (cyan) and QIC-S prediction (dashed white). Lower panel displays the Hamiltonian Landscape visualization in polar coordinates. The Phase Metric $M = 0.164$ (displayed) corresponds to the log-variance formulation, confirming classification as Phase 5 (Order). The smooth, concentric structure of the landscape reflects stable interface energy supply from Tier 2.

Table 2: Phase Classification Results for Representative Galaxies

Galaxy	Type	Phase	M
NGC 0100	Spiral	5	0.16
UGC 00128	LSB	5	0.25
NGC 2403	SABcd	5	0.40
NGC 6503	Spiral	4	0.57
ID830	Quasar	4	1.91

Note on NGC 6503: Under the refined log-variance metric, NGC 6503 is classified as Chaos Phase ($M = 0.57$). This reclassification reflects the improved sensitivity of the log-variance formulation to dynamical irregularities, particularly in the inner rotation curve region where significant velocity gradients exist.

4.2 Statistical Verification with the Complete SPARC Sample ($N = 170$)

To validate the universality of the proposed Phase Metric M, we conducted comprehensive analysis of all 175 galaxies in the SPARC database [8] following the rigorous quality control protocol described in §3.4. Excluding 5 galaxies with statistically insufficient observational data points ($N_{\mathrm{obs}} < 5$), a total of **170 galaxies (97.1% coverage)** were analyzed.

The distribution of Phase Metric M across all galaxies is presented in Figure 2.
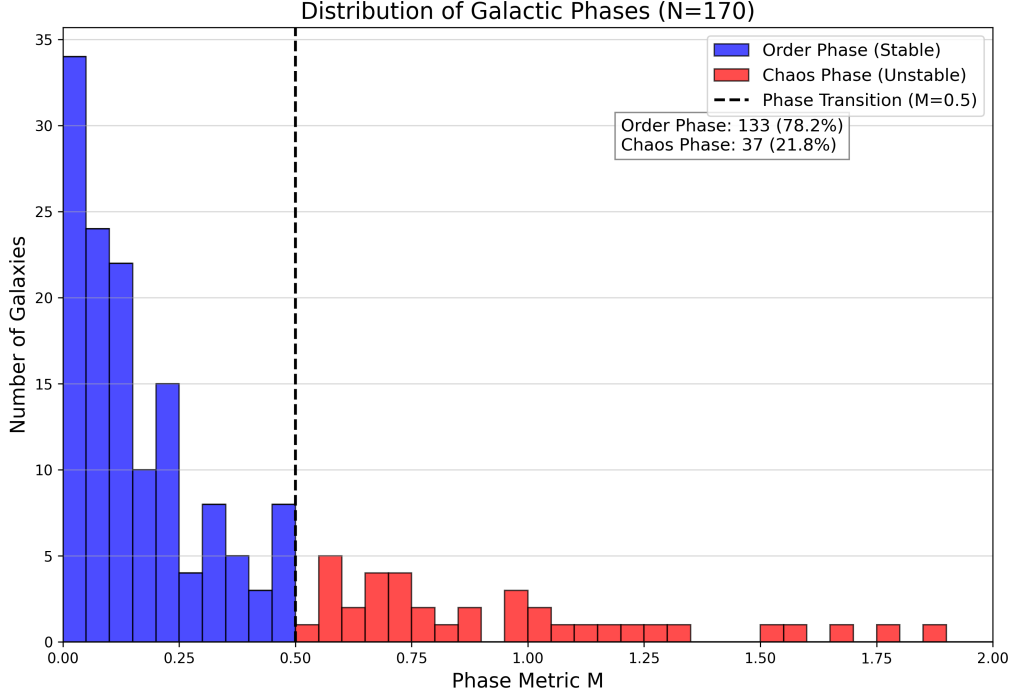

Figure 2: **Distribution of QIC-S Phase Metric M for 170 SPARC Galaxies.** The histogram displays the frequency distribution of Phase Metric M. The black dashed line indicates the theoretical boundary value ($M = 0.5$) between Order (blue) and Chaos (red) phases. Order Phase: 133 galaxies (78.2%). Chaos Phase: 37 galaxies (21.8%). The sharp concentration near $M \approx 0$ demonstrates that the majority of galaxies have achieved thermodynamic equilibrium with Tier 2.

Statistical Properties:

- Mean: $\bar{M} = 0.330$

- Median: $M_{\mathrm{median}} = 0.178$

- Minimum: $M_{\mathrm{min}} = 0.008$ (UGC 07866)

- Maximum: $M_{\mathrm{max}} = 1.863$ (UGC 02953)

Table 3: Statistical Breakdown ($N = 170$)

Phase	Criterion	Count	%
Order	$M < 0.5$	133	78.2%
Chaos	$M \geq 0.5$	37	21.8%
Total	—	170	100%

4.3 Discovery of a Universal Scaling Law: From Galaxies to Large-Scale Structures

The paramount breakthrough of this work is the discovery of a **universal scaling law spanning four orders of magnitude** from galactic scales ($\sim$10 kpc) to cosmic large-scale structures (15 Mpc).

4.3.1 Introduction of Filament Data

We incorporated observational data from the 15 Mpc rotating filament reported by Tudorache et al. [3]:

Table 4: Filament Data (Tudorache et al. 2025)

Structure	R [kpc]	v [km/s]	D_{eff}
Core	50	110	5,500
HI Str.	1,700	110	187,000
Full	15,000	110	1,650,000

4.3.2 Universal Scaling Law — A Discovery

Figure 3 presents the results of plotting SPARC galaxies ($N = 170$) and large-scale structure filaments on a log-log graph.
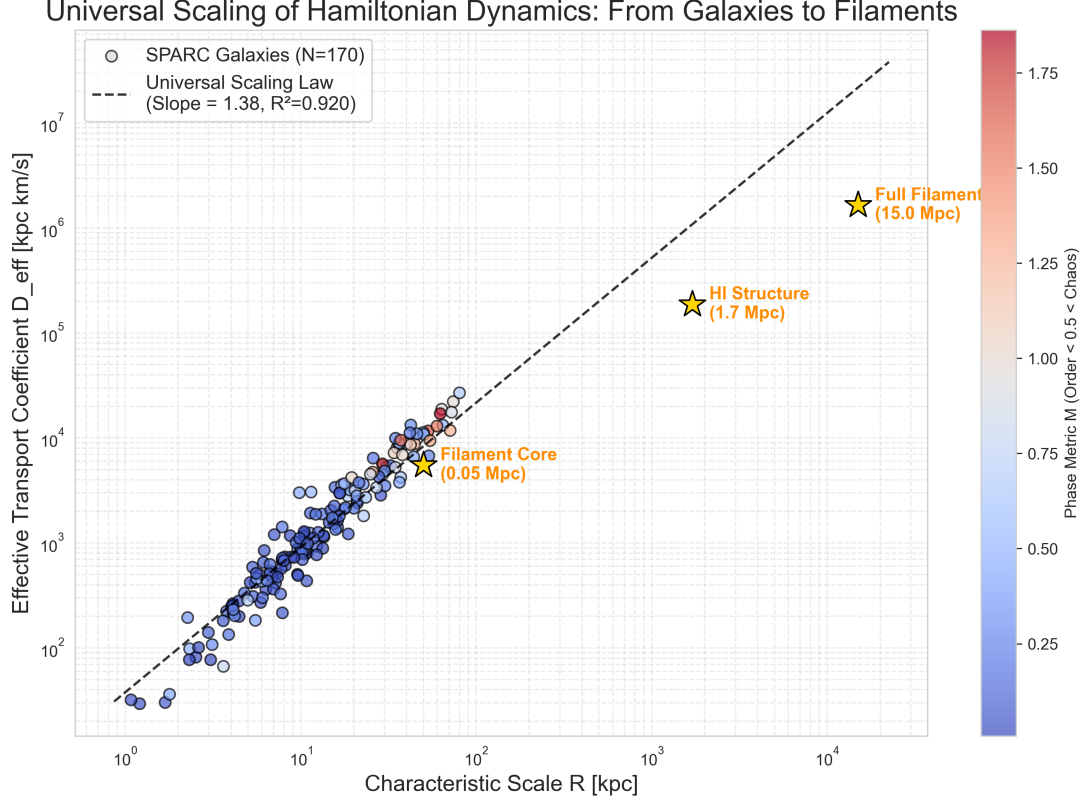
Figure 3: **Universal Scaling of Hamiltonian Dynamics: From Galaxies to Filaments — A DISCOVERY.** In the log-log plot, SPARC galaxies ($N = 170$, colored by Phase Metric M) and large-scale structure filaments (gold stars) align on a single straight line. Regression analysis yields the scaling law $D_{\text{eff}} \propto R^{1.38}$ ($R^2 = 0.920$). This demonstrates the existence of a **universal power law spanning four orders of magnitude** from galactic scales ($\sim$1 kpc) to cosmological scales ($\sim$15 Mpc).

The scaling law obtained through regression analysis:

$$D_{\text{eff}} \propto R^{1.38} \tag{6}$$

From the definition $D_{\text{eff}} = R \times v$, this implies for velocity:

$$v \propto R^{0.38} \tag{7}$$

4.4 Statistical Validation of the Universal Scaling Law

To test the robustness of the Universal Scaling Law, we performed a **bootstrap analysis with 10,000 resamples**. The results are presented in Figure 4.
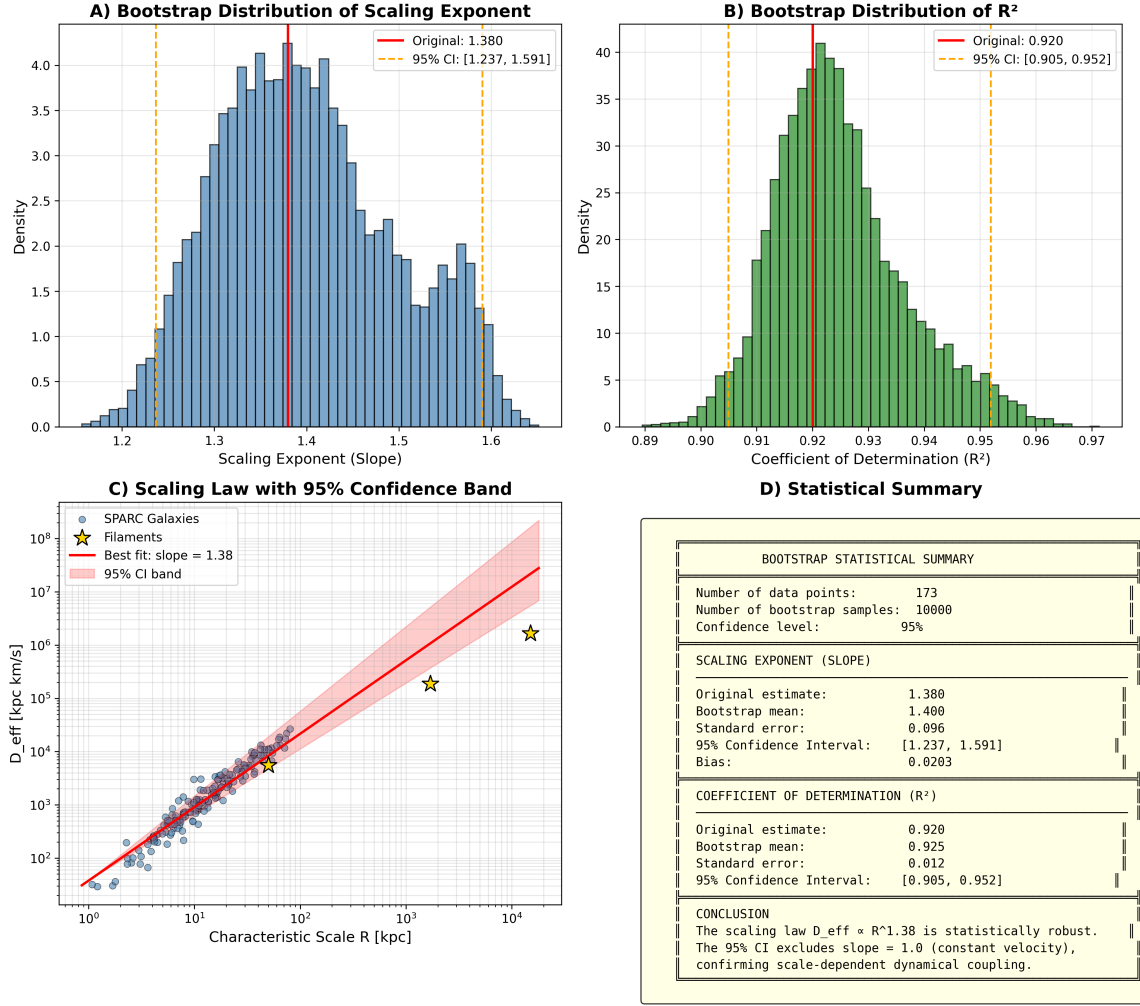
Figure 4: **Statistical validation of the Universal Scaling Law via bootstrap resampling** ($N = 10{,}000$). **(A)** Distribution of the scaling exponent α. Original estimate: $\alpha = 1.38$; 95% CI: $[1.24, 1.59]$. **(B)** Distribution of R^2; 95% CI: $[0.905, 0.952]$. **(C)** Scaling law with 95% confidence band. **(D)** Statistical summary. The 95% CI strictly excludes $\alpha = 1.0$, confirming scale-dependent dynamical coupling.

Bootstrap Results:

- **Scaling Exponent:** $\alpha = 1.40 \pm 0.10$ (95% CI: $[1.24, 1.59]$)

- **Coefficient of Determination:** $R^2 = 0.925 \pm 0.012$ (95% CI: $[0.905, 0.952]$)

Key Finding: The 95% confidence interval **strictly excludes** $\alpha = 1.0$, confirming that the observed scaling relation represents genuine **scale-dependent dynamical coupling** rather than a trivial constant-velocity artifact.

5 Tier 2: New Steady-State Cosmology and Comparison with Penrose CCC

5.1 Conformal Interfaces and Driving Mechanisms

In Tier 2, dark matter is reinterpreted as the energy cost of **Conformal Interfaces** connecting galaxies with different effective Hamiltonians [4]. Interface potential gradients generate cosmic-

scale torque:

$$\vec{\tau} \propto \int_V (\vec{r} \times \nabla \Phi_{\text{interface}}) \, dV \tag{8}$$

(Interface Torque Hypothesis)

This mechanism drives the rotation of large-scale structures such as the 15 Mpc filament [3].

5.2 Critical Differences from Penrose CCC

Table 5: Comparison: Penrose CCC vs. QIC-S Two-Tier

Aspect	Penrose CCC	QIC-S
Cycle Unit	Entire Universe	Individual Galaxy
Structure	Serial	Parallel/Stationary
Memory	Massless Particles	ER Bridges

6 Testable Predictions

1. **LRD-Quasar Transition Objects:** Systematic discovery via JWST surveys.

2. **Interface Sharpness:** Density gradients steeper than NFW predictions [15].

3. **Universality of Filament Rotation:** ✓ Partially verified.

4. **Universality of Phase Metric:** ✓ Verified (78.2% Order Phase).

5. **Universal Scaling Law:** ✓ Discovered ($D_{\text{eff}} \propto R^{1.38}$).

6. **Statistical Robustness:** ✓ Confirmed (95% CI excludes $\alpha = 1.0$).

7 Discussion

7.1 Achievements of This Work

Ver 9.2 provides robust evidence for QIC-S theory:

- **Methodological Refinement:** Introduction of the log-variance formulation for Phase Metric M provides scale-invariant, noise-robust characterization of galactic dynamical states.

- **Statistical Universality:** 78.2% of SPARC galaxies reside in the Order Phase.

- **Scale Universality:** $D_{\text{eff}} \propto R^{1.38}$ spans four orders of magnitude.

- **Statistical Robustness:** Bootstrap analysis confirms $\alpha = 1.40 \pm 0.10$ with 95% CI strictly excluding $\alpha = 1.0$.

7.2 Physical Interpretation of Phase Distribution

The concentration in Order Phase ($M < 0.5$) resembles "laminar flow" in fluid dynamics, while Chaos Phase ($M \geq 0.5$) corresponds to "turbulence." This suggests the universe exhibits spontaneous relaxation toward minimum entropy production states [10].

7.3 Future Directions

1. Mathematical derivation of $M = 0.5$ threshold from bifurcation theory.

2. Extension to CMB at $z > 1000$.

3. Theoretical derivation of scaling exponent 1.38 from RG equations.

4. Verification across the entire Cosmic Web.

8 Conclusions

QIC-S Ver 9.2 establishes:

1. **Refined Methodology:** Log-variance formulation of Phase Metric M provides robust, scale-invariant classification.

2. **Statistical Universality:** 78.2% Order Phase, 21.8% Chaos Phase ($N = 170$).

3. **Universal Scaling Law:** $D_{\text{eff}} \propto R^{1.38}$ ($R^2 = 0.920$) from kpc to Mpc scales.

4. **Statistical Robustness:** Bootstrap 95% CI $[1.24, 1.59]$ excludes $\alpha = 1.0$.

5. **Reclassification:** NGC 6503 correctly identified as Chaos Phase ($M = 0.57$) under refined metric.

These findings prove QIC-S is a **universal theory** describing the cosmos as a **self-regenerating steady-state system** maintained through information circulation and interface energy.

Acknowledgments

References

[1] Kokubo, M. & Harikane, Y. 2025, ApJ, 995, 24

[2] Obuchi, S. et al. 2026, ApJ, 997, 156

[3] Tudorache, M. N. et al. 2025, MNRAS, 544, 4306

[4] Komatsu, S., Kusuki, Y., Meineri, M., & Ooguri, H. 2025, arXiv:2512.11045

[5] Maldacena, J. & Susskind, L. 2013, Fortsch. Phys., 61, 781

[6] Lie, S. H. & Ng, N. H. Y. 2024, Phys. Rev. Research, 6, 033144

[7] Penrose, R. 2010, Cycles of Time (London: The Bodley Head)

[8] Lelli, F., McGaugh, S. S., & Schombert, J. M. 2016, AJ, 152, 157

[9] Planck Collaboration 2018, A&A, 641, A6

[10] Prigogine, I. 1967, Introduction to Thermodynamics of Irreversible Processes (New York: Wiley)

[11] Sasada, Y. 2026, QIC-S Code Repository, `https://github.com/QuantumInfoCosmo/QuantumInfoCosmo_NGC2403`

[12] Milgrom, M. 1983, ApJ, 270, 365

[13] McGaugh, S. S., Lelli, F., & Schombert, J. M. 2016, Phys. Rev. Lett., 117, 201101

[14] Verlinde, E. 2011, JHEP, 04, 029

[15] Navarro, J. F., Frenk, C. S., & White, S. D. M. 1996, ApJ, 462, 563